Available online at www.sciencedirect.com
SCIENCE DIRECT®
Journal of Molecular Catalysis A: Chemical 221 (2004) 155–162
JOURNAL OF MOLECULAR CATALYSIS A: CHEMICAL
www.elsevier.com/locate/molcata

NCO adsorption over SiO_2 and Cu/SiO_2 cluster models from density functional theory

Ricardo M. Ferullo, Norberto J. Castellani*

Grupo de Materiales y Sistemas Catalíticos, Departamento de Física, Universidad Nacional del Sur, Av. Alem 1253, 8000 Bahía Blanca, Argentina

Received 4 May 2004; received in revised form 29 June 2004; accepted 30 June 2004
Available online 12 August 2004

Abstract

The adsorption of NCO over two types of surface defects on silica surface, ≡Si• and ≡Si–O•, were studied using the density functional theory formalism. The adsorption is preferred on ≡Si• site in agreement with experimental results. The NCO adsorption is also studied over atomic and dimer copper deposited on silica defects and, for comparison reasons, on free Cu and Cu_2. While in the first case the support does not affect the Cu–NCO bonding, it enhances that interaction in the second case. This behaviour is related to the higher charge transfer from the dimer to NCO, which produces a strong Cu–NCO bonding which has an important ionic character. Besides, the adsorbate modifies the metal–support interaction due to an electrostatic bond enhancement between the terminal Cu atom and a regular bridging O atom of the silica surface. The NCO asymmetric stretching frequencies were also calculated and analysed.

Keywords: NCO adsorption; Cu/SiO_2; Cu catalysts; Metal–support interaction; Density functional theory

1. Introduction

The reduction of NO_x over metal catalysts is of great importance for removal of pollutant gases from vehicle exhausts. The typical reductants of NO_x are CO, H_2 and hydrocarbons. Particularly, the NO/CO reaction was extensively studied in the past [1–10]. In this reaction the NO molecule decomposes on the metal surface. The N atoms can then recombine to N_2. At the same time, adsorbed CO is oxidized to yield CO_2.

The study of the behavior of NCO is of interest because it may play a major role in the undesirable formation of C_2N_2 and HCN molecules during the catalytic treatment of automobile exhaust gases [11]. In an earlier work, Unland observed the formation of the isocyanate (NCO) surface complex during NO/CO reactions on a series of oxide-supported metal catalysts [1]. Later, Solymosi et al. studying Pt supported over different oxides concluded that NCO is localized on the support rather than on the metallic phase [2]. Noticeably, in the absence of metal catalyst this species is not detected on any of the oxides usually used as supports [12]. Thus, the NCO is formed on the metal and then migrates onto the support. There, it can accumulate to a large extent yielding an intense infrared absorption band due to its asymmetric stretching mode. The NCO species has also been observed in the catalytic reduction of NO by non-saturated hydrocarbons and in NH_3/CO reactions [13–15]. Although for many years the NCO was considered as a spectator species, very recently some experimental studies performed over Rh/TiO_2, Pd/Al_2O_3 and Cu/Al_2O_3 systems suggest that it could act as an intermediate in the production of N_2O or N_2 [9,10,13].

The activity of Cu-containing catalysts has been examined for the catalytic reduction of NO_x [13,14,16]. These catalysts are being studied as a possible alternative facing supported Rh systems for oxide nitrogen reduction reactions. When a NO/CO equimolar mixture is adsorbed on reduced Cu/SiO_2 catalysts at room temperature the formation of CO_2, N_2O and NCO is observed [4]. Solymosi and Bánsági studied the

* Corresponding author. Tel.: +54 291 4595141; fax: +54 291 4595142.
E-mail addresses: caferull@criba.edu.ar (R.M. Ferullo), castella@criba.edu.ar (N.J. Castellani).

1381-1169/$ – see front matter © 2004 Elsevier B.V. All rights reserved.
doi:10.1016/j.molcata.2004.06.027

behavior of the NCO species on different Cu/SiO_2 catalysts by adsorbing isocyanic acid (HNCO) [17]. Using infrared (IR) spectroscopy they observed the characteristic band at 2230–2240 cm^{-1} due to the asymmetric stretching mode of NCO adsorbed on metallic Cu and at 2300 cm^{-1} when this group adsorbs on silica in reduced Cu/SiO_2 samples. Besides, the stability of the NCO over Cu/SiO_2 resulted to be very high in comparison with silica-supported Pt and Rh catalysts. In the latter systems NCO migrated to the support or decomposes to N_2 and CO when the temperature increases and, as a result, no NCO was detected above 300 K. Conversely, it disappears completely only above 473 K on supported Cu catalysts.

Recently, Boccuzzi et al. have characterized reduced Cu/SiO_2 catalysts by using infrared spectroscopy of adsorbed CO [7]. One of the bands located at about 2130 cm^{-1} could be interpreted as the presence of a polarized species due to an electric field generated by $Cu^{\delta+}$ centers. Thus, the authors assigned this band to Cu isolated atoms and small two-dimensional Cu particles slightly positively charged by the interaction with the support [7,18]. Besides, these two-dimensional aggregates were very active for the CO–NO reaction.

Metal–support interactions have been studied in the past for several systems and strong changes in the electronic structure of the metal have been observed. In this context, quantum-chemical studies of the interaction between gas molecules and supported small metallic particles are essential to get an accurate description of adsorption processes and they constitute a very useful tool for the understanding of the catalytic activity of supported metal systems.

The study of the metal/oxide interface represents a field of wide interest because it involves a variety of technical applications in catalysis, gas sensors, electrochemistry, microelectronics, etc. In particular, in heterogeneous catalysis the oxide acts as a support where the metal particle grows. Nevertheless, it is largely known that the reactivity of the metal is modified by the effect of the support. Despite the importance of this subject, at the present there are relatively few theoretical articles devoted to the interaction of small metallic particles with oxides like SiO_2 and Al_2O_3. This is probably due to the lack of accurate experimental information about metal–oxide interface. Recently, Lopez et al. investigated several aspects of Cu deposition on silica. Using a DFT method they found that the regular sites of the silica surface are unreactive toward the metal atoms. In contrast, defect sites like $\equiv Si^{\bullet}$ and $\equiv Si{-}O^{\bullet}$ (the $\equiv$ symbol indicates the three Si–O bonds) are very reactive and they are probably centers where the nucleation takes place [19]. Using Cu_n clusters (n = 1–5) they observed that the partial charge transfer to the oxide favors the formation of electrostatic interactions between the Cu aggregates and the non-defective two-coordinated O atoms of the silica surface [20]. Later, the same authors showed that while the free Cu clusters are unreactive toward H_2 dissociation, the supported clusters exhibit a high reactivity that is connected with a strong rearrangement of the metal structure [21].

In this study a theoretical analysis of the NCO adsorption on defect sites of pure silica and on Cu_n (n = 1, 2) particles supported on silica is performed in the framework of density functional theory (DFT). The goal of this work is to attain a qualitative understanding of the influence of silica on NCO–metal interaction. This will be done mainly by comparing the results of binding energies and vibrational frequencies for the different adsorbed species and by analyzing the corresponding electronic charge distributions.

2. Theoretical considerations and surface models

The calculations of this work have been performed within the density functional theory (DFT) using the hybrid B3LYP exchange-correlation functional [22] as implemented in the software package Gaussian 98 [23]. This method has been widely used for adsorption processes yielding reliable results both on oxides and metal clusters [24–28]. Thus, the results corresponding to atomic Cu and Pd adsorption on other oxides as MgO show that highly correlated conventional quantum-chemical calculations (couple cluster techniques) and the hybrid B3LYP-DFT approach give very similar results for the metal/oxide bond [28]. On the other hand, gradient-corrected functionals such as BPW91 and BP86 yield larger binding energies. In the case of B3LYP method used for metal/oxide systems the dependence on the size ba-

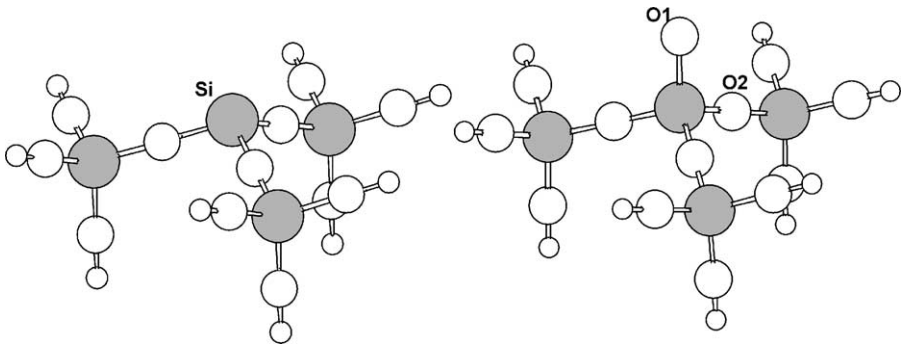

Fig. 1. Schematic representation of the $\equiv Si{-}^{\bullet}$ (left) and $\equiv Si{-}O^{\bullet}$ (right) defects on the silica cluster model.

sis set is not extremely critical. It was observed a variation of nearly 0.08 eV in the binding energy when a triple-zeta basis is compared with a double-zeta one [28].

The SiO_2(1 1 1) surfaces were represented using $Si_4O_3(OH)_9$ and $Si_4O_4(OH)_9$ clusters following the ideal β-cristobalite structure (see Fig. 1). The terminal oxygen atoms were saturated with hydrogens. It is a well-known procedure to embed the cluster and so to eliminate spurious effects due to the dangling bonds. The geometric structure of the oxide was fixed throughout the calculation. In particular, the Si–O and the O–H distances were set to 1.61 and 0.98 Å, respectively. The distances, angles and dihedral angles for adsorbed species over the defective sites of the support were fully optimized.

The molecular orbitals were expanded using the 6-31G basis set on O, Si, C, N and H atoms. For Cu, we used an effective core potential with a [8s5p5d/3s3p2d] basis set for the $3s^2 3p^6 3d^{10} 4s^1$ valence electrons [29]. Polarization functions were added to those atoms directly involved in the geometrical optimization. The atomic charges were calculated by using the natural bond orbital (NBO) population analysis [30]. The spin density (SD) is expressed in terms of the Mülliken population analysis [31].

The adsorption energies (E_{ads}) were computed as the difference between the energy of the NCO/substrate system and the sum of the energies of the separated fragments. The full counterpoise procedure was applied to correct the basis set superposition error (BSSE) [32].

3. Results and discussion

3.1. NCO adsorption on SiO_2

It has been suggested that the ≡Si• and ≡Si–O• sites (the so-called E' and nonbridging oxygen centers, respectively) are very reactive to gas molecules and metal aggregates, and that they could be the primary origin of the interface bond formation [33]. These centers are characterized by the presence of an unpaired electron on the Si and O atoms, respectively, and for this reason they are detectable by electron paramagnetic resonance (EPR) spectroscopy. Indeed, as it can be observed in Table 1, the calculations give a spin density strongly concentrated on Si (0.86) at the ≡Si• site and on O (0.96) at the ≡Si–O• site. The positive Si charge in the ≡Si–O• defect (+2.47e) is practically the same than at SiO_4 tetrahedron without defects (+2.45e) and is considerably larger than in the ≡Si• defect (+1.94e). The amount of negative charge of the oxygen atom at the ≡Si–O• center (−0.59e) is much smaller than that of a regular bridging oxygen in the silica surface (−1.26e).

Table 1
Si–O distance (in Å), NBO net charges (in electron units) and spin density (SD) for ≡Si• and ≡Si–O• defect sites at the silica surface

	≡Si•	≡Si–O•
d(Si–O1)	–	1.677
q(Si)	+1.94	+2.47
q(O1)	–	−0.59
q(O2)	−1.28	−1.26
SD	0.86 (Si)	0.96 (O)

Next, the interaction of the NCO group with both silica defects, ≡Si• and ≡Si–O•, was studied (see Fig. 2). The most important geometrical, energetic and vibrational properties have been summarized in Table 2, together with the atomic NBO charges of different atoms participating of this interaction. The corresponding values for the isocyanic acid (HNCO), bearing also the NCO group, have been included. The adsorption energy values indicate that the NCO adsorbs much strongly on ≡Si• centers. This is in agreement with the IR spectra recorded during NO/CO reactions on silica-supported metal transition catalysts where the feature at 2300 cm^{-1} was assigned to the ≡Si–NCO species [3,17]. As the unpaired electron at free NCO is largely localized concentrated on the N atom (the corresponding spin density value is 0.73), so the interaction occurs between two open-shell fragments yielding a very strong covalent bond. Notice that it was determined that the stability of NCO on silica is higher than on other oxides usually used as supports like alumina and titania [17]. In addition, our calculations reveal that the adsorption on the ≡Si–O• site is also possible with an energy value of ∼2 eV which is still in the range of chemisorption

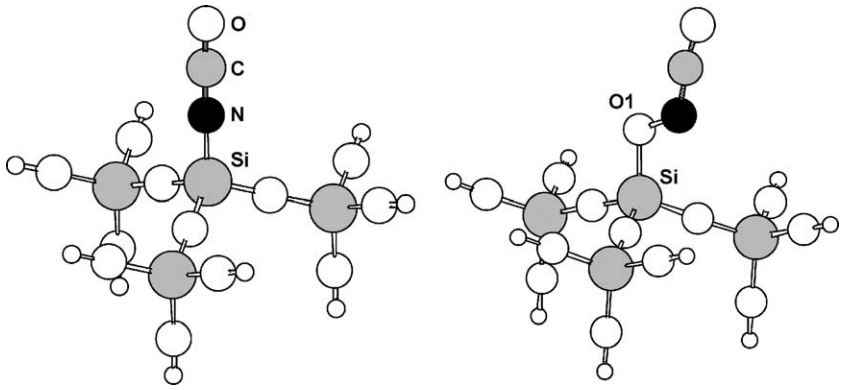

Fig. 2. Schematic representation of the NCO adsorption on ≡Si• (left) and ≡Si–O• (right) defects.

Table 2
Optimized distances (in Å), NBO net charges (in electron units), adhesion energies (in eV) and the NCO asymmetric stretching mode frequency (in cm^{-1}) for the isocyanic acid molecule and the NCO adsorption over silica defects

	HNCO	≡Si─NCO	≡Si─O─NCO
d(N─Si)	–	1.708	–
d(N─O1)	–	–	1.409
d(N─C)	1.218	1.197	1.230
d(C─O)	1.175	1.181	1.177
q(Si)	–	+2.52	+2.56
q(O1)	–	–	−0.70
q(N)	−0.79	−0.99	−0.31
q(C)	+0.86	+0.90	+0.84
q(O)	−0.50	−0.53	−0.48
q(NCO)	−0.43	−0.62	+0.05
E_{ads}	–	−5.20 (−5.44)	−2.22 (−2.38)
ν(NCO)	2266	2346	2203

Values in parenthesis are the adsorption energy without the BSSE correction.

bonding. Unfortunately, at the present enough accurate IR studies of NCO adsorption over silica at low temperatures have not been published in order to confirm that such adsorbed state does exist. The distance between N and O atoms in the SiO–NCO bond is ∼17% elongated with respect to the typical N–O distance (∼1.2 Å). In spite of being ≡Si–O• and NCO two open-shell species, their interaction is not too strong likely to the fact that the atoms involved in the bond, N and O, are negatively charged.

Looking at the NBO charges in Tables 1 and 2 we can infer that when NCO adsorbs on ≡Si• a significant charge transfer of nearly 0.6e is produced from the Si site to the NCO group. Over the other site, ≡Si–O•, both Si and O charges vary slightly comparing before and after the NCO adsorption takes place, due to a negligible charge transfer between NCO and the oxide surface. Concerning the NCO asymmetric stretching mode frequency, our calculated value when NCO adsorbs on ≡Si• shows an overestimation of only 46 cm^{-1} with respect to the experimental one (2300 cm^{-1}, see above). In the case of NCO adsorption on ≡Si–O·this frequency is about 140 cm^{-1} lower than that for the more stable adsorption site ≡Si•.

Table 3
Optimized distances (in Å), NBO net charges (in electron units), spin densities (SD) and adhesion and nucleation energies (in eV) for copper atom and dimer adsorptions over ≡Si• defect

	≡Si─Cu_1	≡Si─Cu_2
d(Si─Cu1)	2.273	2.324
d(Cu─Cu)	–	2.352
q(Si)	+1.90	+1.88
q(Cu2)	+0.04	+0.07
q(Cu2)	–	−0.03
SD(Si)	–	0.21
SD(Cu1)	–	0.14
SD(Cu2)	–	0.59
E_{adh} (eV)	−2.10 (−2.51)	−1.02 (−1.37)
E_{nucl} (eV)	–	−0.62 (−0.88)

Values in parenthesis are the corresponding energies without the BSSE correction.

3.2. *Cu and Cu_2 deposition on SiO_2*

First, in Table 3 the results corresponding to the deposition of Cu monomer and dimer over ≡Si• site are shown. In both cases a weak charge transfer occurs from the metal to the support. When the dimer is adsorbed on this silica defect, a bending of Cu_2 is produced yielding a Si–Cu–Cu angle of 112° (see Fig. 3). The Cu–Cu distance becomes greater by 4% than that obtained for the dimer at gas phase (2.260 Å). The calculation of the spin density distribution for Cu_2–Si≡ which is an open-shell system shows that the unpaired electron is mainly concentrated at the dimer, particularly at the terminal Cu atom.

The adhesion energy E_{adh} defined as $E_{adh} = [E(Cu_n/SiO_2) - E(Cu_n) - E(SiO_2)]$, with n = 1 or 2, has been computed considering the total energy E for the optimized supported clusters with respect to the isolated fragments. Their values are reported in Table 3. Notice that E_{adh} for Cu_1 is higher in magnitude by about 1 eV than E_{adh} for Cu_2. As it was clearly discussed by López et al., the adsorption of Cu clusters with an odd-number of electrons is a more favorable situation than that for the clusters with an even-number of electrons because the first ones are open-shell systems and a direct coupling with the unpaired electron of the silica defect is produced. On the contrary, a closed-shell system such as

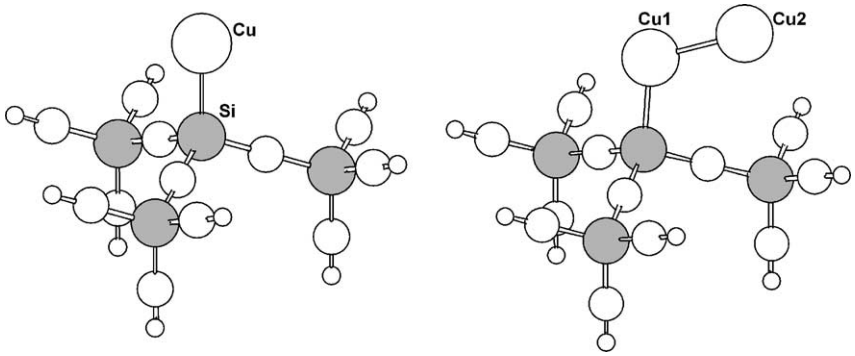

Fig. 3. Model of a supported Cu (left) and Cu_2 (right) on a ≡Si• center at the silica surface.

Table 4
As Table 3 for copper atom and dimer adsorptions over ≡Si–O• defect

	≡Si–O–Cu_1	≡Si–O–Cu_2
d(Si–O1)	1.632	1.627
d(O1–Cu)	1.808	1.843
d(Cu–Cu)	–	2.320
q(Si)	+2.50	+2.49
q(O1)	−1.22	−1.22
q(Cu1)	+0.68	+0.47
q(Cu2)	–	+0.19
q(O2)	−1.28	−1.29
q(O3)	−1.16	−1.17
SD(O1)	–	0.18
SD(Cu1)	–	0.43
SD(Cu2)	–	0.36
E_{adh} (eV)	−2.83 (−3.13)	−2.03 (−2.56)
E_{nucl} (eV)	–	−0.99 (−1.46)

Cu_2 has to "open" its configuration in order to form a covalent bond with the silica defect [20]. Another quantity of interest that we can define is the nucleation energy (E_{nucl}), defined as the energy gain due to the deposition of a Cu atom to a preexistent Cu_n cluster: $E_{nucl} = [E(Cu_n/SiO_2) - E(Cu) - E(Cu_{n-1}/SiO_2)]$ [20]. This energy is relatively low in magnitude because the Cu atom interacts with ≡Si–Cu_1 which is a closed-shell system after the mononer adsorption.

The results concerning the adsorption of the Cu atom and the dimer on the ≡Si–O• defect are summarized in Table 4. The Cu atom is anchored to the silica defect forming a Si–O–Cu angle of 117° (see Fig. 4). An important electron charge transfer occurs from the metal to the support, leaving the metal with a charge of nearly +0.7e. This charge is taken mainly by the O atom of the ≡Si–O• defect. Indeed, the charge of this O atom varies from −0.59e for the isolated defect to −1.22e when the Cu atom is linked to it.

The dimer adsorbs on the ≡Si–O• defect bended towards the surface. The terminal Cu atom approaches to a regular bridging O atom (labeled as O3 in Fig. 4) keeping at a distance of 2.282 Å. As in the case of ≡Si–O–Cu_1 system, for ≡Si–O–Cu_2 a similar amount of electron charge transfer from the metal cluster is produced. The spin density values for Cu_2–O–Si≡ show that the unpaired electron is homogenously distributed between both metal atoms. Notice that the electrostatic interaction that takes place between the positively charged Cu_2 atom and the negatively charged O3 atom could explain the above commented metallic dimer bending. These type of interactions were theoretically predicted even with larger Cu clusters on silica [20]. Such cycles involving metal ions and regular oxygen atoms have recently observed on Ni/SiO_2 systems using extended X-ray absorption fine structure (EXAFS) spectroscopy [34]. Thus, two different O–Cu bonds are formed when the Cu_2 dimer interacts with a defective silica surface, one concerning the O atom of the defect and the other a regular bridging O atom. The corresponding interatomic distances (1.843 and 2.282 Å, respectively) indicate that the first bond is mostly polar covalent and the second mostly electrostatic [20].

The adhesion energy for Cu_2 over the ≡Si–O• defect is about 1 eV higher in magnitude than that over the ≡Si• defect. Therefore, the ≡Si–O• defects are more reactive to both Cu and Cu_2 deposits. However the relative order of the adhesion energies for Cu and Cu_2 over the ≡Si–O• defect is analogous to that obtained over the ≡Si• defect. The Cu nucleation energy is about 0.4 eV greater over the ≡Si–O• defect. In the next section the interaction of the NCO group with ≡Si–O–Cu_1 and ≡Si–O–Cu_2 centers is analysed.

3.3. NCO adsorption on Cu_1/SiO_2 and Cu_2/SiO_2

In Tables 5 and 6 several relevant geometrical, electronic and energetic molecular properties are summarized for the NCO adsorption on ≡Si–O–Cu_1 and ≡Si–O–Cu_2 systems, respectively. As comparison, the same properties for the Cu_n–NCO molecules (n = 1, 2) are included.

Looking at Fig. 5 we observe that the NCO molecule adsorbs directly on the supported Cu atom forming a lineal O–Cu–N–C–O structure. Conversely, when NCO is linked to an isolated Cu atom a Cu–N–C angle of 131° is defined, retaining in the NCO group its linearity. From the results of Table 5 we observe that all the interatomic distances Cu–N, N–C and C–O decrease in the presence of the support; thus, CuNCO acts as a more compact group. The interaction of

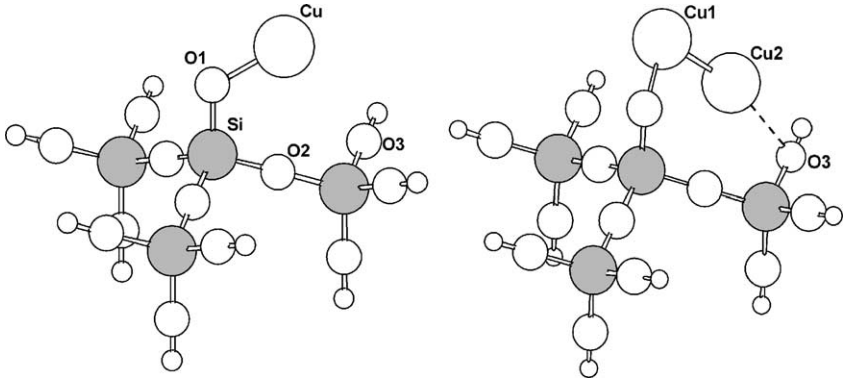

Fig. 4. Model of a supported Cu (left) and Cu_2 (right) on a ≡Si–O• center. The dotted line indicates the electrostatic interaction with a bridging oxygen atom of the silica surface.

Table 5
Optimized distances (in Å), NBO net charges (in electron units), spin densities (SD), adsorption energy (in eV) and NCO asymmetric stretching mode frequency (in cm^{-1}) for NCO adsorption on supported and unsupported Cu atom

	≡Si–O–Cu_1–NCO	Cu_1–NCO
d(Si–O1)	1.654	–
d(O1–Cu)	1.760	–
d(Cu–N)	1.797	1.825
d(N–C)	1.206	1.215
d(C–O)	1.186	1.188
q(Si)	+2.52	–
q(O1)	−1.09	–
q(Cu)	+1.06	+0.71
q(N)	−0.90	−0.94
q(C)	+0.82	+0.78
q(O)	−0.51	−0.55
q(NCO)	−0.59	−0.71
SD	0.34 (O1), 0.37 (Cu), 0.17 (N), 0.11 (O)	–
E_{ads} (eV)	−2.77 (−2.94)	−3.06 (−3.22)

Values in parenthesis are the adsorption energy without the BSSE correction.

Table 6
Optimized distances (in Å), NBO net charges (in electron units), spin densities (SD), adsorption energy (in eV) and NCO asymmetric stretching mode frequency (in cm^{-1}) for NCO adsorption on supported and unsupported Cu dimer

	≡Si–O–Cu_2–NCO	Cu_2–NCO
d(Si–O1)	1.618	–
d(O1–Cu)	1.819	–
d(Cu–Cu)	2.437	2.427
d(Cu1–N)	1.926	1.986
d(Cu2–N)	1.941	1.986
d(N–C)	1.214	1.217
d(C–O)	1.183	1.183
q(Si)	+2.48	–
q(O1)	−1.26	–
q(Cu1)	+0.73	+0.40
q(Cu2)	+0.72	+0.40
q(O2)	−1.28	–
q(O3)	−1.17	–
q(N)	−1.06	−1.11
q(C)	+0.84	+0.84
q(O)	−0.53	−0.53
q(NCO)	−0.75	−0.80
SD	–	0.92 (Cu_2)
E_{ads} (eV)	−4.31 (−4.56)	−2.19 (−2.40)

Values in parenthesis are the adsorption energy without the BSSE correction.

this group with the ≡Si–O• site is accompanied with an electron transfer from the silica O atom as it was the situation for ≡Si–O–Cu_1. Nevertheless, the amount of this transfer is somewhat smaller (0.5e versus 0.6e).

Considering the interaction of the NCO group with supported Cu atom an important charge transfer of about 0.6e occurs from the CuO fragment to the NCO. In the case of the Cu_1–NCO molecule this effect is slightly greater (∼0.7e). According to these observations the isocyanate group acts as a $NCO^{\delta-}$ species when it is adsorbed on supported Cu_1 system, producing a covalent bond with a strong polar character. A similar situation occurs with the Cu_1–NCO molecule. Regarding the adsorption energies as a measure of the bond between adsorbate and substrate is clear that the effect of the support is negligible in the NCO–Cu_1 interaction. In the case of supported Cu_1–NCO system the spin density values show that the unpaired electron is localized largely on the CuO fragment (SD = 0.7), becoming this group an active site for later adsorptions. Thus, as a consequence of this charge transfer the unpaired electron present at free NCO before adsorption pairs with another electron partially "closing" the originally open NCO high orbital. On the other hand, after adsorption an unpaired electron remains mostly located at the support.

Concerning the NCO interaction with the supported Cu dimer, the NCO adsorption in bridge retains the linear geometry for NCO as it can be deduced looking at Fig. 5. Moreover, from Table 6 we observe that after NCO adsorption the Cu–Cu distance increases by about 0.12 Å with respect to the supported Cu dimer. The charge that the NCO group receives is higher (by 0.15e) than that for supported Cu atom. The

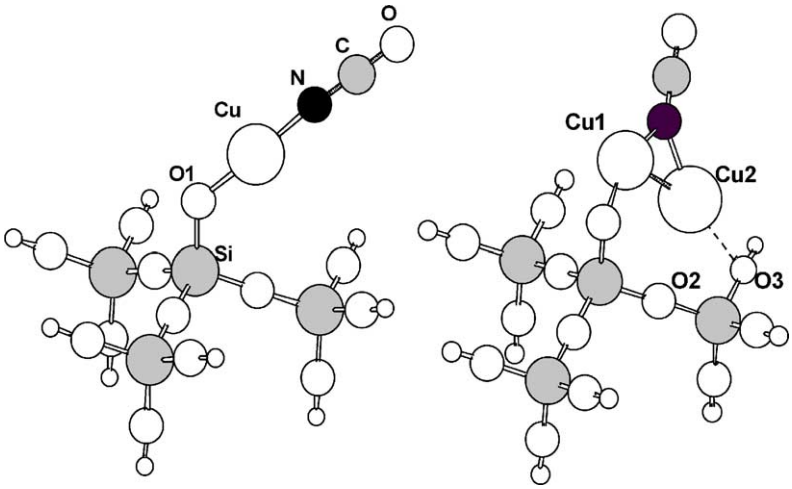

Fig. 5. Schematic representation of NCO adsorption on silica-supported Cu (left) and Cu_2 (right).

Table 7
NCO asymmetric stretching frequencies (in cm^{-1}) for the NCO adsorption on silica, supported Cu atom, supported Cu dimer, free Cu atom and free Cu dimer[a]

	≡Si–NCO	≡SiOCu$_1$NCO	≡SiOCu$_2$NCO	Cu$_1$–NCO	Cu$_2$–NCO
Calculated	2346	2218	2230	2193	2209
Experimental	2300	2180–2220; 2230–2240[b]		–	–

[a] Scaled according to the empirical factor of 0.9613 as suggested in Ref. [23].
[b] Assigned to ν(NCO) for the NCO adsorption on reduced Cu/SiO_2 catalysts. From Refs. [7,17], respectively.

charge of the dimer increases from +0.66e to +1.45e after NCO adsorption. This electron loss is higher than in the case of the supported Cu_1 system (0.79e versus 0.38e). Because of that, the NCO charge is higher in the case of the dimer (−0.75 versus −0.59). The excess of negative charge is mainly concentrated in the N atom. This fact, together with the higher positive charge of the metal, indicates that in the dimer case a more relevant polarization effect on the Cu–NCO interaction is present. On the other hand, the important increase of the terminal Cu positive charge should produce an enhancement of the electrostatic attraction between this Cu atom and the regular bridging O atom, shortening the distance between them from 2.282 Å (without NCO) to 2.122 Å (with NCO). In other words, we have an example where the adsorbed group is able to modify the proper metal–support properties.

Regarding the nature of the metal–NCO interaction, some experimental and theoretical studies have suggested that the NCO acts as ionic rather than a neutral species, in line with the present calculations. Hecker and Bell compared the NCO asymmetric stretching frequencies observed on supported Rh catalysts with those reported for transition metal complexes. They noted that the values for adsorbed NCO were more in line with negatively charged complexes than with neutral ones, suggesting that the species might be partially charged and, in this case, they should be written as $Rh–NCO^{\delta-}$ [3]. In addition, Yang and Whitten showed from ab initio dipole moment calculations that the NCO bonding to Ni(1 0 0) surface is largely ionic [35].

The NCO adsorption over the isolated Cu_2 dimer also produces an important charge transfer from the dimer to the isocyanate (by 0.80e). Here the spin density calculations show a system with the unpaired electron almost concentrated on the dimer. But this electron cannot be shared with the support and therefore the Cu atoms acquire a much lower positive charge than in the supported Cu_2 dimer. As a consequence, the Cu_2–NCO interaction becomes weaker. From the NCO adsorption energy values we infer that NCO is linked to the metal particle very strongly in the supported Cu_2 system due to the important positive charge of Cu atoms. Moreover, the enhancement of the dimer-support interaction, through the terminal Cu and the regular bridging O atom, contributes to the global stabilization. The high value of the NCO adsorption is compatible with the small capability of NCO to migrate on Cu in comparison with other metals such as Rh and Pt [17]. However, since the NCO adsorption energy on ≡Si• defect is significantly higher (∼1 eV) than that of supported Cu we infer that NCO could migrate from the metal to the support, in agreement with experiments.

Notice in addition that the NCO asymmetric stretching frequencies are about 20 cm^{-1} higher for the supported systems than for the isolated ones. The corresponding values for the NCO adsorption over ≡Si–O–Cu_1 and ≡Si–O–Cu_2 centers (2218 and 2230 cm^{-1}) are in good agreement with the experimental data for reduced Cu/SiO_2 catalysts (see Table 7).

4. Conclusions

i) The NCO group adsorbs stronger over ≡Si• site than over ≡Si–O• site. In the former case a relevant charge transfer of 0.6e is produced from the silica site to NCO.
ii) The ≡Si–O• site is more reactive than ≡Si• site for the interaction with copper. In the first case the bond is accompanied with an important charge transfer from the metal to the support. This charge is taken mainly by the O atom of the ≡Si–O• defect. In the case of the ≡Si–O–Cu_2 system the terminal Cu atom interacts electrostatically to a regular bridged O atom of the silica surface.
iii) NCO adsorbs strongly on ≡Si–O–Cu_n (n = 1, 2) sites. This fact is likely related to the small capability of NCO to migrate on Cu. Supported copper behaves as an electron source to both the support and the adsorbate. The NCO group acts as NCO^- ion rather than a neutral species. The support does not affect the NCO adsorption on monomer Cu, but it has a positive effect on the dimer adsorption capability. This behaviour is related to the higher charge transfer from the dimer to NCO, which produces a strong Cu–NCO bonding which has an important ionic character. The presence of the adsorbate enhances the Cu interaction with a regular bridging O atom at the silica surface.

Acknowledgements

Financial support from CONICET and UNS are gratefully acknowledged.

References

[1] M.L. Unland, J. Catal. 31 (1973) 459.
[2] F. Solymosi, L. Völgyesi, J. Sárkány, J. Catal. 54 (1978) 336.
[3] W.C. Hecker, A.T. Bell, J. Catal. 85 (1984) 389.
[4] A.R. Balkenende, G.J.G. van der Grift, E.A. Meulenkamp, J.W. Geus, Appl. Surf. Sci. 68 (1993) 161.
[5] H. Permana, K.Y. Simon Ng, C.H.F. Peden, S.J. Schmieg, D.K. Lambert, D.N. Belton, J. Catal. 164 (1996) 194.

[6] V.P. Zhdanov, B. Kasemo, Surf. Sci. Rep. 29 (1997) 31.
[7] F. Boccuzzi, S. Coluccia, G. Martra, N. Ravasio, J. Catal. 184 (1999) 316.
[8] A.M. Venecia, L.F. Liotta, G. Deganello, P. Terreros, M.A. Peña, J.L.G. Fierro, Langmuir 15 (1999) 1176.
[9] D. Kondarides, T. Chafik, X. Verykios, J. Catal. 193 (2000) 303.
[10] A.M. Sica, C.E. Gigola, Appl. Catal. A 239 (2003) 121.
[11] R.J.H. Voorhoeve, C.K.N. Patel, L.E. Trimble, R.J. Kerl, J. Catal. 54 (1978) 102.
[12] F. Solymosi, T. Bánsági, J. Phys. Chem. 83 (1979) 552.
[13] K. Shimizu, H. Kawabata, H. Maeshima, A. Satsuma, T. Hattori, J. Phys. Chem. B 104 (2000) 2885.
[14] Y. Chi, S.S.C. Chuang, J. Catal. 190 (2000) 75.
[15] D.K. Paul, C.D. Marten, Langmuir 14 (1998) 3820.
[16] J. Shibata, K. Shimizu, A. Satsuma, T. Hattori, Appl. Catal. B 37 (2002) 197.
[17] F. Solymosi, T. Bánsági, J. Catal. 156 (1995) 75.
[18] F. Boccuzzi, A. Chiorino, G. Martra, M. Gargano, N. Ravasio, B. Carrozzini, J. Catal. 165 (1997) 129.
[19] N. López, F. Illas, G. Pacchioni, J. Am. Chem. Soc. 121 (1999) 813.
[20] N. López, F. Illas, G. Pacchioni, J. Phys. Chem. B 103 (1999) 1712.
[21] N. López, F. Illas, G. Pacchioni, J. Phys. Chem. B 103 (1999) 8552.
[22] A.D. Becke, J. Chem. Phys. 98 (1993) 5648.
[23] M.J. Frisch, G.W. Trucks, H.B. Schlegel, G.E. Scuseria, M.A. Robb, J.R. Cheeseman, V.G. Zakrzewski, J.A. Montgomery, R.E. Stratmann, J.C. Burant, S. Dapprich, J.M. Millam, A.D. Daniels, K.N. Kudin, M.C. Strain, O. Farkas, J. Tomasi, V. Barone, M. Cossi, R. Cammi, B. Mennucci, C. Pomelli, C. Adamo, S. Clifford, J. Ochterski, G.A. Petersson, P.Y. Ayala, Q. Cui, K. Morokuma, D.K. Malick, A.D. Rabuck, K. Raghavachari, J.B. Foresman, J. Cioslowski, J.V. Ortiz, B.B. Stefanov, G. Liu, A. Liashenko, P. Piskorz, I. Komaromi, R. Gomperts, R. L. Martin, D.J. Fox, T. Kieth, M.A. Al-Laham, C.Y. Peng, A. Nanayakkara, C. Gonzalez, M. Challacombe, P.M.W. Gill, B.G. Johnson, W. Chen, M.W. Wong, J.L. Andres, M. Head-Gordon, E.S. Replogle, J.A. Pople, Gaussian 98 (Revision A.7), Gaussian, Inc., Pittsburgh, PA, 1998.
[24] R. Soave, G. Pacchioni, Chem. Phys. Lett. 320 (2000) 345.
[25] M.M. Branda, C. Di Valentin, G. Pacchioni, J. Phys. Chem. B 108 (2004) 4752.
[26] Q. Cui, D.G. Musaev, K. Morokuma, J. Phys. Chem. A 102 (1998) 6373.
[27] R.M. Ferullo, N.J. Castellani, J. Mol. Catal. A: Chem. 212 (2004) 359.
[28] N. López, F. Illas, N. Rösch, G. Pacchioni, J. Chem. Phys. 110 (1999) 4873.
[29] P.J. Hay, W.R. Wadt, J. Chem. Phys. 82 (1985) 299.
[30] A.E. Reed, L.A. Curtiss, F. Weinhold, Chem. Rev. 88 (1988) 899.
[31] I.N. Levine, Quantum Chemistry, 5th ed., Prentice Hall, New Jersey, 2000.
[32] N.R. Kestner, J.E. Combariza, Reviews in Computational Chemistry, Wiley–VCH, John Wiley and Sons Inc, New York, 1999, Chap. 2.
[33] J.B. Zhou, H.C. Lu, T. Gustafsson, E. Garfunkel, Surf. Sci. Lett. 293 (1993) 887.
[34] J.Y. Carriat, M. Che, M. Kermarec, M. Verdaguer, A. Michalowicz, J. Am. Chem. Soc. 120 (1998) 2059.
[35] H. Yang, J.L. Whitten, Surf. Sci. 401 (1998) 312.